ICDERS

27th

International Colloquium on the Dynamics of Explosions and Reactive Systems

Sunday 28th July
-
Friday 2nd August 2019

Beijing, China

Topic	Detonation Failure/Limits	RDE 1	Ignition 2	Dynamics & Stability 2	Energetic Materials 2
13:50	**Critical Ignition in Detonation Cells due to Expansion Cooling(319)** *K. Cheevers, R. Murugesan, F. Giroux, W. Morin, A. Dion-Dallaire, M. Radulescu*	**Characterization of Detonation Wave Heat Release and Rotating Detonation Engine Mode Selection(351)** *J. Burr, K. Yu*	**Rapid compression machine (RCM) studies on the production of unsaturated hydrocarbons from methane(257)** *S. Drost, R. Schie?l, U. Maas*	**Large Eddy Simulations of turbulent premixed flame stabilization by pulsed plasma discharges(171)** *Y. Bechane, N. Darabiha, V. Moureau, C. Laux, B. Fiorina*	**A spectroscopic method for assessing the degree of oxidation of zirconium-based pyrotechnic initiators(112)** *J. Ryu, J. Yoh*
14:15	**Propagation limit of gaseous detonations governed by yielding con?nement and Arrhenius kinetics(359)** *L. Zhou, X. Mi, H.D. Ng, Y. Zhang, H. Teng*	**Detonation Propagation in a Linear Representation of a Rotating Detonation Engine(384)** *C. Metrow, G. Ciccarelli*	**Effects of NTC region on end-gas combustion modes under temperature stratification(266)** *T. Nogawa, H. Terashima*	**Numerical studies of the flame dynamics in a novel, ultra-lean, non-premixed model GT burner using PDF-ESF method(76)** *S. Yu*	**The changes of thermodynamic reactions of a NASA standard initiator due to hygrothermal aging(113)** *J. Oh, Y. Park, J. Yoh*

The changes of thermodynamic reactions of pyrotechnic initiator ZPP by hygrothermal aging effects

Juyoung Oh[1], Seung-gyo Jang[2], Jack J. Yoh[1]
[1]Department of Mechanical and Aerospace Engineering, Seoul National University
Seoul, Korea 151-742
[2]Agency for Defense Development
Daejeon, Korea 34060

1 Introduction

When energetic materials are in storage for a long period of time, the performance degradation may occur due to various factors such as oxidization, hydrolysis, chemical or structural deformations. Various studies have investigated the accelerated aging researches for energetic materials to obtain the aging effects and estimate the lifespan of the aged samples in reduced time [1, 2]. However, the relative humidity (RH) should be considered essentially in aging analysis to replicate the aging influences in real environments. Although propellant or explosive substances are kept hermetically sealed, during the sealing process, they cannot help exposing to external environment [3]. Furthermore, the degraded sealing system may arise when the device is stored for a lengthy period of time. Thus, the current study provides the aging effects of energetic materials, which varied with both RH and temperature conditions, to provide the various and detailed results reflecting the actual environment.

The aging analysis was conducted for Zirconium Potassium Perchlorate (ZPP), utilized universally as a NASA Standard Initiator (NSI) [4]. ZPP consists of zirconium (Zr) as a fuel, potassium perchlorate ($KClO_4$) as an oxidant, and Viton b as a binder. Actually, prior study investigated the ZPP aging to reveal the extreme humidity effect on aging only [5]. The present research applied aging conditions in a variety of RH (0, 30%, 70%, and 100%) to ZPP samples. The authors also newly provide the surface analysis showing chemical variations in both fuel (Zr) and oxidants ($KClO_4$) by utilizing X-ray photoelectron spectroscopy (XPS). Moreover, the thermal analysis and reaction kinetics were extracted from the differential scanning calorimetry (DSC). The extracted kinetics were also utilized in simulating the trend of reaction progress for ZPPs aged with various aging conditions. The simulation result matched with conducted experimental results very well. Thus, it can be derived the fact that the high-RH conditions significantly cause the ZPP performance degradation.

2 Experimental details and kinetics calculations

Correspondence to: jjyoh@snu.ac.kr

2.1 Materials

The ZPP materials, a powdery form, consists of 52 wt% Zr (Rockwood Lithium, ~2 μm, USA), 42 wt% $KClO_4$ (Barium & Chemical Inc., ~6 μm, USA), 5 wt% Viton b ($[-C_7H_2F_{12}-]_n$) (Dupont, USA) and 1 wt% graphite. Prior to conducting the DSC experiment, each sample was sifted through a 200 mesh (75 μm) particle sieve. The utilized ZPP samples were aged at 71°C following aerospace guidelines [2] at various RH levels for different aging periods. Henceforth, each sample will be referred by the sample labels represented in Table 1.

Table 1: Sample list and aging conditions under which the ZPP samples were aged.

Sample label	Aging conditions			Utilized for XPS	Aging type
	Temperature (°C)	Relative humidity	Aging duration		
0	-	-	-	O	Unaged
1	71	0%	4 months	O	Thermal
2	71	0%	8 months	O	Thermal
3	71	30%	2 weeks	O	Hygrothermal
4	71	30%	8 weeks	O	Hygrothermal
5	71	70%	2 weeks	O	Hygrothermal
6	71	70%	8 weeks	O	Hygrothermal
7	71	100%	2 weeks	O	Hygrothermal
8	71	100%	4 weeks	O	Hygrothermal
9	71	100%	6 weeks	-	Hygrothermal

2.2 XPS study

Ultra-high-vacuum (UHV) AXIS-SUPRA (Kratos, UK) was employed to measure the ZPP mixtures' chemical bonding state, relative quantification, and detailed XPS spectra. This apparatus is equipped with micro focused monochromatized Al Kα X-ray sources (1486.6 eV) and a hemispherical analyser (WX-600). The base pressure in the sample analysis chamber and the load lock chamber was less than $5*10^{-10}$, and $5*10^{-8}$ torr, respectively.

2.3 DSC study and peak deconvolution method

The DSC experiments were carried out using the DSC-3+ instrument from Mettler Toledo. The materials were heated from 30 to 600 ℃ with the slow heating rates (1, 2, 3, and 4 ℃/min) and 85 ml/min nitrogen atmosphere to observe the thermal reaction process obviously. At least three replicates were performed for each sample, and the proper sample weight about 2-3 mg was predicted, which can inhibit the heating rate effect. The materials were distributed evenly over the bottom of standard 40 μm pierced aluminium pan to avoid the concentrated heat inside the pan and were sealed. To provide the reasonable kinetic analysis, the DSC data were collected following the International Confederation for Thermal Analysis and Calorimetry (ICTAC) Kinetics Committee's recommendations [6].

The overlapping exothermic reactions can be separated into sub-reactions using the Fraser-Suzuki function, installed in AKTS (Advanced Kinetics and Technology Solutions) software program [7]. The peak deconvolution method was applied to the reaction rate-temperature relationship of ZPP sample heated at 3 °C/min, which was obtained from the process of kinetic analysis.

2.4 Reaction kinetics calculations based on Friedman-isoconversional method

In the current study, the activation energy was calculated by utilizing the AKTS software program. The kinetic parameters such as activation energy (E_α) and pre-exponential factor (A_α) were obtained using the Friedman-isoconversional method [8]. The current study restricted the range of the reaction progress (α) to 0.2–0.8 to reflect the range where high accuracy of calculation is included.

3 Results

3.1 XPS-DSC analysis

Figure 1(a) represents the variation of the fuel composition. In the XPS result, zirconium dioxide (ZrO_2) signals (182.20 and 184.50 eV) are presented instead of Zr signal because Zr is spontaneously covered with a thin oxide layer when it is exposed to external environment due to its reactive and sensitive characteristic [9]. The XPS result shows the increase of ZrO_2 signals in aged samples, signifying that ZPP can be affected by either oxygen in the air or oxidants when it ages. The ZrO_2 content increased rapidly with the RH level.

In case of surface analysis for the oxidant, small portion of potassium chlorate ($KClO_3$) was identified even though the unaged ZPP sample was composed of $KClO_4$ with high purity (≥ 99%). Therefore, the relationship between $KClO_3$ (206.50 eV) and $KClO_4$ (208.70 eV) was addressed in the current study. As Fig. 1(b) shows, the composition of the $KClO_4$ also varied according to each RH condition. In the thermal aging case, $KClO_4$ decomposed into $KClO_3$ while the hygrothermal aging cases had different patterns. 30% RH cannot be discovered any significant effect on the ZPP composition compared to the unaged sample while in cases of 70% and 100% RH, both $KClO_4$ and $KClO_3$ decomposed rapidly.

The differences in the DSC thermograms also occurred clearly between the unaged (Fig. 2(a)) and aged ZPP sample (Fig. 2(b)). The sample 0 consists of one endothermic peak and broad exothermic peaks. The endothermic reaction at 300°C indicates the phase transition of $KClO_4$ [1]. The exothermic reactions around 350~500°C represent the combustion reaction between fuel and oxidizer [10]. Meanwhile, Fig. 2(b), the sample 9 shows a new exothermic peak around 500°C. This reaction resulted from the hygrothermal aging effect, which causes the increased amount of ZrO_2 that cannot function as a reducing agent. Thus, the decomposition of remaining $KClO_4$ [1] in Sample 9 was identified by DSC thermograms.

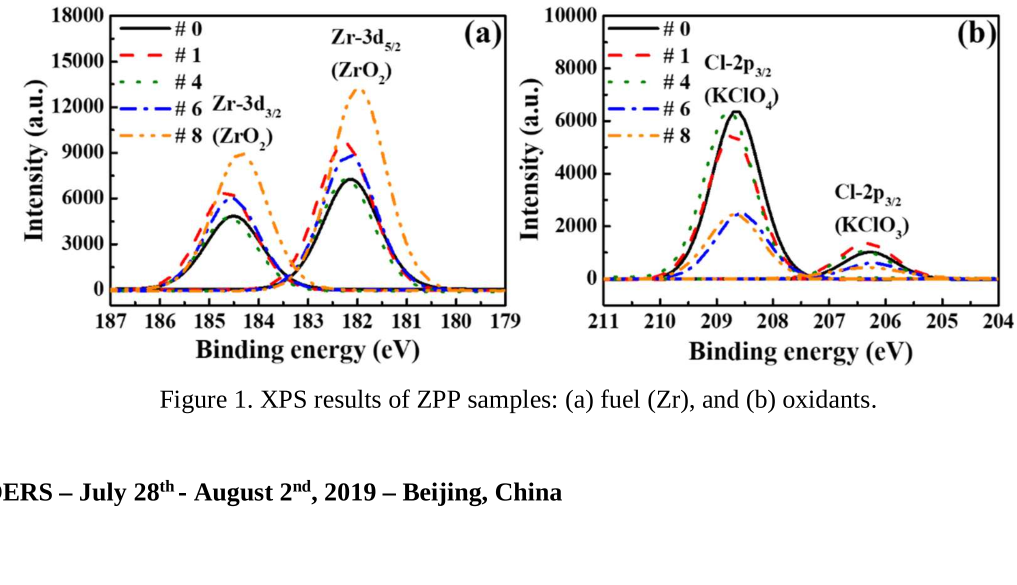

Figure 1. XPS results of ZPP samples: (a) fuel (Zr), and (b) oxidants.

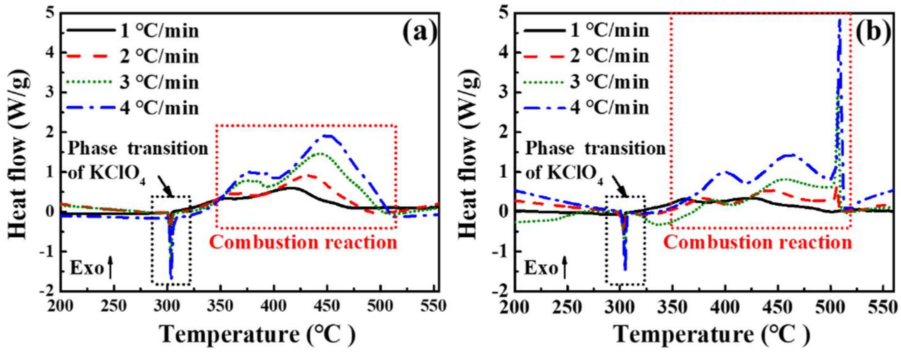

Figure 2. DSC results of ZPP samples: (a) unaged ZPP (sample 0) and (b) hygrothermally aged ZPP (sample 9).

3.2 Peak deconvolution analysis on the basis of DSC thermograms

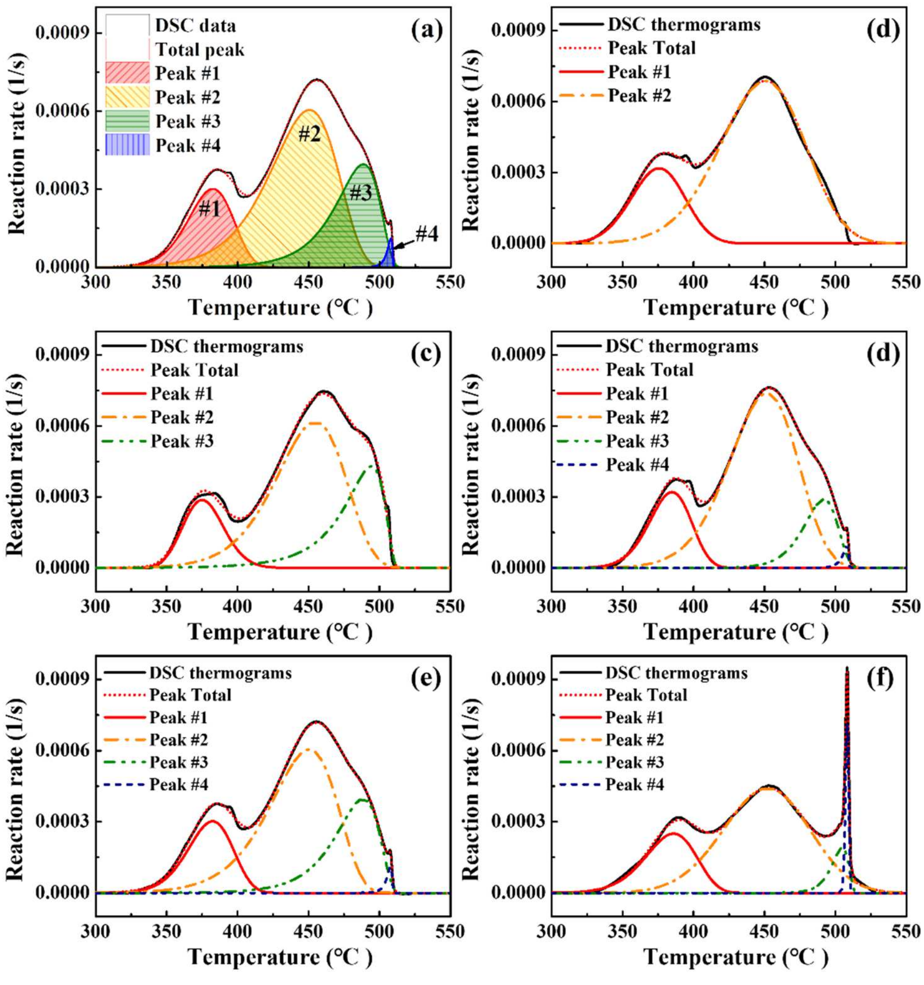

Figure 3. Peak deconvolution results of ZPP samples: (a) the illustration of overall reaction composition, (b) unaged, (c) thermal aging (0% RH), (d) 30% RH condition, (e) 70% RH condition, and (f) 100% RH condition.

To examine the detailed aging effects to the exothermic reactions, peak deconvolution analysis was conducted. Based on the previous studies, the whole combustion reaction of ZPP is considered to be comprised of four sub-reactions [1, 10, 11], namely combustion reactions among Viton b, Zr, $KClO_3$ and $KClO_4$ (Peak 1), combustion reactions among Zr, $KClO_3$ and $KClO_4$ (Peak 2), $KClO_3$ decomposition reaction (Peak 3), and $KClO_4$ decomposition reaction (Peak 4) as shown in Fig. 3(a). Figure 3 shows the results for between unaged and both thermal and hygrothermal aging cases. The thermal aging case included the three exothermic reactions (Peaks 1, 2 and 3). Among these reactions, $KClO_3$ decomposition (Peak 3) stood out in comparison with the sample 0. The result was also in accordance with the XPS result (Fig. 1(b)). As Figs. 3(d-f) show, all four exothermic reactions composed the combustion process of hygrothermally aged ZPP. Figure 3(d) and 3(e), ZPPs aged under 30% and 70% RH conditions, show nearly analogous to the results of the thermal aging case. 100% RH case, however, was different remarkably. Here, the remained $KClO_4$ decomposition, the result from the considerably increased ZrO_2 content, was particularly magnified.

3.3 Reaction kinetics based on Friedman-isoconversional analysis and simulation of the ZPP reaction progress

Figure 4(a) shows both the heat of reaction (ΔH) with errors, range of E_α and average E_α value for all ZPP samples. The ΔH decreased as the aging period was longer while the E_α had opposite trend. Even though the hygrothermally aging was applied to ZPP samples for only a few weeks, the reaction enthalpy values were similar to those of the thermal aging cases. Thus, it is fairly likely that the RH level leads a significant decrease in the heat of reaction. The E_α of the sample aged under low-RH condition for a long period decreased continually. As can be seen in Fig. 1(b), this can be attributed to $KClO_3$, an intermediate reaction product, which is more reactive and sensitive than $KClO_4$ [12]. Under high-RH conditions (Samples 5-9), E_α tended to increase with each RH level. The increasing trend can be derived from the aging effect, namely the growth of ZrO_2, which is in stable state resulting in the insensitive ZPP.

Figure 4(b) shows the reaction progress from unreacted (α = 0) to completely reacted (α = 1) calculated based on the kinetic parameters obtained from DSC experiments. The Arrhenius equation which is solved for various aging cases can be represented as,

$$\frac{d\alpha}{dt} = A_\alpha \exp(-\frac{E_\alpha}{RT_\alpha}) \quad (1)$$

where R, T_α are the universal gas constant and temperature (in K) at the corresponding α, respectively.

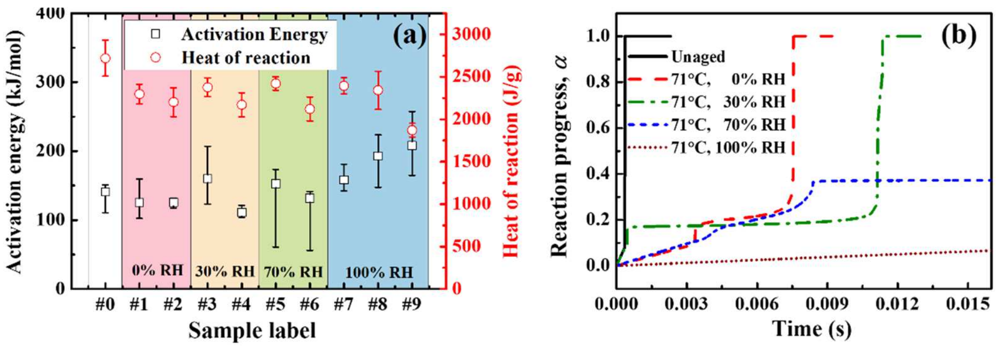

Figure 4. (a) Variation in activation energy values and heats of reaction for various aging types, and (b) calculated reaction of each representative ZPP samples for each aging type.

In this simulation of constant volume reaction for ZPP, specific heat and density at constant pressure are taken as 250 J/kg-K and 4600 kg/m^3, respectively. The samples are ensured to ignite promptly at 1100 K, a preheated value, and observed to progress into a complete reaction. As represented, the more delayed conversion rate was observed at extreme hygrothermal aging types. Especially, 70% RH condition occurred a misfire or incomplete reaction at about 35% conversion, and 100% RH case failed to react.

ACKNOWLEDGMENTS

This work was financially supported by Korea National Research Foundation under the National Space Laboratory Program 2014 (NRF-2014M1A3A3A02034903) through IAAT at Seoul National University. Additional funding came from the Advanced Research Center (NRF-2013R1A5A1073861) contracted through the Next Generation Space Propulsion Research Center at Seoul National University. Yoonsik Park performed the numerical simulation of the aging samples.

References

[1] Sorensen DN, Quebral AP, Baroody EE, Sanborn WB. (2006). Investigation of the thermal degradation of the aged pyrotechnic titanium hydride/potassium perchlorate. J. Therm. Anal. Calorim. 85: 151.

[2] Kim Y, Ambekar A, Yoh JJ. (2017). Toward understanding the aging effect of energetic materials via advanced isoconversional decomposition kinetics. J. Therm. Anal. Calorim. 133: 737.

[3] Lee J, Kim T, Ryu SU, Choi K, Ahn GH, Paik JG, Ryu BT, Park TH, Won YS. (2018). Study on the Aging Mechanism of Boron Potassium Nitrate ($BKNO_3$) for Sustainable Efficiency in Pyrotechnic Mechanical Devices. Scientific reports. 8:11745.

[4] Bement LJ. (1999). Multhaup HA. Determining functional reliability of pyrotechnic mechanical devices. AIAA J. 37: 357.

[5] Lee J, Choi KW, Ryu SU, Ahn GH, Paik JG, Ryu BT, Won YS. (2018). Aging Mechanism of Zirconium Potassium Perchlorate Charge in Pyrotechnic Mechanical Devices. Nanosci. Nanotech. Let. 10: 735.

[6] Vyazovkin S, Chrissafis K, Di Lorenzo ML, Koga N, Pijolat M, Roduit B, Sbirrazzuoli N, Suñol JJ, (2014). ICTAC Kinetics Committee recommendations for collecting experimental thermal analysis data for kinetic computations. Thermochim. Acta 590: 1.

[7] AKTS AG, http://www.akts.com. AKTS-Thermokinetics software.

[8] Friedman HL. (1964). Kinetics of thermal degradation of char-forming plastics from thermogravimetry. Application to a phenolic plastic. J. Polym. Sci., Polym. Symp. 6: 183.

[9] Brochu M, Gauntt BD, Boyer L, Loehman RE. (2009). Pressureless reactive sintering of ZrB2 ceramic. J. Eur. Ceram. Soc. 29: 1493.

[10] Lu KT, Yang CC. (2008). Thermal Analysis Studies on the Slow-Propagation Tungsten Type Delay Composition System. Propellants Explos. Pyrotech. 33: 403.

[11] Ravanbod M, Pouretedal HR, Amini MK, Ebadpour R. (2016). Kinetic study of the thermal decomposition of potassium chlorate using the non-isothermal TG/DSC technique. Cent. Eur. J. Energ. Mat. 13: 505.

[12] Shamsipur M, Pourmortazavi SM, Fathollahi M. (2012). Kinetic parameters of binary iron/oxidant pyrolants. J. Energ. Mater. 30: 97.